Available online at www.sciencedirect.com
SCIENCE DIRECT
Scripta Materialia 54 (2006) 931–935
Scripta MATERIALIA
www.actamat-journals.com

Phase transformations in a Cu–25at.%Al–7.5at.%Mn alloy

S.Y. Yang, T.F. Liu *

Department of Materials Science and Engineering, National Chiao Tung University, 1001 Ta Hsueh Road, Hsinchu 30049, Taiwan, ROC

Received 24 August 2005; received in revised form 30 September 2005; accepted 27 October 2005
Available online 29 November 2005

Abstract

The as-quenched microstructure of the Cu–25at.%Al–7.5at.%Mn alloy was $D0_3$ phase containing extremely fine L–J precipitates (the L–J phase is a new type of precipitate, which was firstly observed and identified by Liu and Jeng (designated L–J phase) in a $Cu_{2.2}$-$Mn_{0.8}Al$ alloy.). When the as-quenched alloy was aged at temperatures ranging from 500 °C to 700 °C, the phase transition sequence was found to be (γ-brass + L–J + $D0_3$) → (γ-brass + L–J + B2) → β. This result is different from that reported by previous workers in Cu–25at.%Al–(0–8)at.%Mn alloys.
© 2005 Acta Materialia Inc. Published by Elsevier Ltd. All rights reserved.

Keywords: Cu–Al–Mn alloy; $D0_3$; L–J phase; γ-brass; B2

1. Introduction

In previous studies, it is seen that when an alloy with a chemical composition in the range of Cu–25at.%Al–(0–8)at.%Mn was solution-treated in single β phase (disordered body-centered cubic) region and then quenched rapidly, a $\beta \rightarrow B2 \rightarrow D0_3$ phase transition occurred during quenching [1–3]. When the as-quenched alloys were aged at temperatures ranging from 350 °C to 600 °C, γ-brass particles were found to appear within the $D0_3$ or B2 matrix [4–6]. The γ-brass has a $D8_3$ (ordered body-centered cubic) structure with lattice parameter $a = 0.872$ nm [7,8], and the orientation relationship between the γ-brass and the matrix was cubic to cubic [9,10]. Based on their studies, it is seen that the stable microstructure of the Cu–25at.%Al–(0–8)at.%Mn alloys as the aging temperature increased changed from (γ-brass + $D0_3$) → (γ-brass + B2) → β. Recently, we made transmission electron microscopy (TEM) observations of the phase transformations of the Cu–25at.%Al–7.5at.%Mn alloy. Consequently, it was found that in the as-quenched condition, the microstructure of the alloy was $D0_3$ phase containing extremely fine L–J precipitates. The L–J phase has an orthorhombic structure with lattice parameters $a = 0.413$ nm, $b = 0.254$ nm and $c = 0.728$ nm [11]. When the as-quenched alloy was aged at temperatures ranging from 500 °C to 700 °C, the phase transition sequence was found to be (γ-brass + L–J + $D0_3$) → (γ-brass + L–J + B2) → β, rather than the (γ-brass + $D0_3$) → (γ-brass + B2) → β reported by previous workers in Cu–25at.%Al–(0–8)at.%Mn alloys.

2. Experimental procedure

The alloy, Cu–25at.%Al–7.5at.%Mn ($Cu_{2.7}Mn_{0.3}Al$), was prepared in a vacuum induction furnace by using 99.9% Cu, 99.9% Al and 99.9% Mn. The melt was chill cast into a $30 \times 50 \times 200$-mm copper mold. After being homogenized at 900 °C for 72 h, the ingot was sectioned into 2.0-mm thick slices. These slices were subsequently solution-treated at 900 °C for 1 h and then quenched into room-temperature water rapidly. The aging processes were performed at temperatures ranging from 500 °C to 700 °C for various times in a vacuum heat-treated furnace and then quenched rapidly.

TEM specimens were prepared by means of a double-jet electropolisher with an electrolyte of 70% methanol and 30% nitric acid. The polishing temperature was kept in

* Corresponding author. Tel.: +886 3 5731675; fax: +886 3 5728504.
E-mail address: tfliu@cc.nctu.edu.tw (T.F. Liu).

1359-6462/$ - see front matter © 2005 Acta Materialia Inc. Published by Elsevier Ltd. All rights reserved.
doi:10.1016/j.scriptamat.2005.10.074

the range from −30 °C to −15 °C, and the current density was kept in the range from 3.0×10^4 A/m^2 to 4.0×10^4 A/m^2. Electron microscopy was performed on a JEOL JEM-2000FX scanning transmission electron microscope operating at 200 kV. This microscope was equipped with a Link ISIS 300 energy-dispersive X-ray spectrometer (EDS) for chemical analysis. Quantitative analyses of elemental concentrations for Cu, Al and Mn were made with the aid of a Cliff–Lorimer ratio thin section method.

3. Results and discussion

Fig. 1(a) is a bright-field (BF) electron micrograph of the as-quenched alloy, showing that a high density of extremely fine precipitates was formed within the matrix. Fig. 1(b) and (c) are two selected-area diffraction patterns (SADPs) of the as-quenched alloy. It is seen in the SADPs that in addition to the reflection spots corresponding to the $D0_3$ phase [12,13], the diffraction patterns also consist of extra spots with streaks caused by the presence of the extremely fine precipitates. When compared with our previous studies in $Cu_{2.2}Mn_{0.8}Al$ and Cu–14.6Al–4.3Ni alloys [11,14], it is found that these extra spots with streaks should belong to the L–J phase with two variants. Fig. 1(d) is a $(\bar{1}\,1\,1)$ $D0_3$ dark-field (DF) electron micrograph of the same area as Fig. 1(a), revealing the presence of the fine $D0_3$ domains with $a/2\langle1\,0\,0\rangle$ anti-phase boundaries (APBs). Fig. 1(e), a $(0\,0\,2)$ $D0_3$ DF electron micrograph, shows the presence of the small B2 domains with $a/4\langle1\,1\,1\rangle$ APBs. In Fig. 1(d) and (e), it is seen that the sizes of both $D0_3$ and B2 domains are very small. Therefore, it is deduced that the $D0_3$ phase existing in the as-quenched alloy was formed by a $\beta \rightarrow B2 \rightarrow D0_3$ continuous ordering transition during quenching [15,16]. Fig. 1(f) is a $(1\,0\,0_1)$ L–J DF electron micrograph, exhibiting the presence of the extremely fine L–J precipitates. Based on the above observations, it is concluded that the as-quenched microstructure of the alloy was $D0_3$ phase containing extremely fine L–J precipitates, where the $D0_3$ phase was formed by the $\beta \rightarrow B2 \rightarrow D0_3$ continuous ordering transition during quenching.

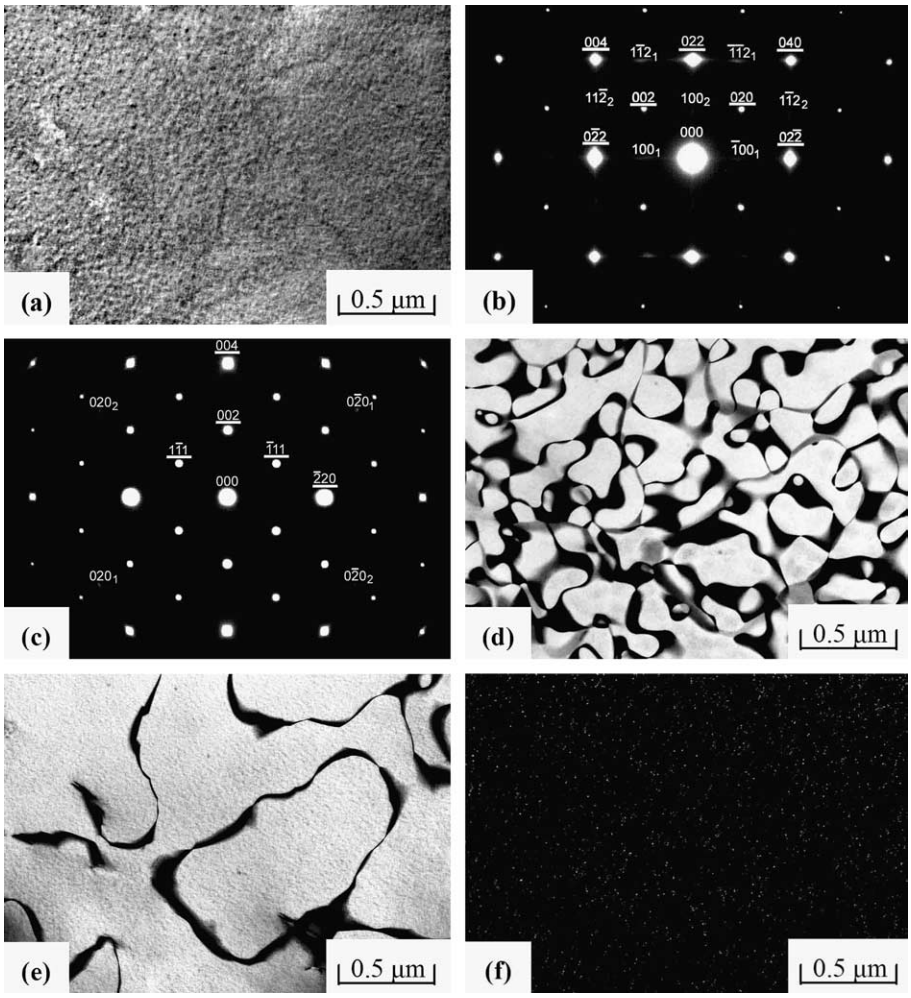

Fig. 1. Electron micrographs of the as-quenched alloy: (a) BF, (b) and (c) two SADPs. The zone axes of the $D0_3$ phase are (b) [1 0 0] and (c) [1 1 0], respectively ($\underline{h\,k\,l} = D0_3$, $hkl_{1,2}$ = L–J phase, 1: variant 1; 2: variant 2), (d) and (e) $(\bar{1}\,1\,1)$ and $(0\,0\,2)$ $D0_3$ DF, respectively, (f) $(1\,0\,0_1)$ L–J DF.

When the as-quenched alloy was aged at 500 °C for moderate times, some coarse particles with a cubic shape started to occur. A typical example is shown in Fig. 2. Fig. 2(a) shows a BF electron micrograph of the alloy aged at 500 °C for 20 min. Electron diffraction demonstrated that the cubic-shaped particles were of γ-brass phase. Fig. 2(b) is an SADP taken from an area covering the particle marked as "R" in Fig. 2(a) and its surrounding matrix. It indicates that the orientation relationship between the γ-brass and the $D0_3$ matrix is $(001)_{\gamma\text{-brass}}\|(001)_m$ and $(010)_{\gamma\text{-brass}}\|(010)_m$, which is similar to that found by previous workers in Cu–Al based alloys [9,10]. Fig. 2(c), a $(\bar{1}11)$ $D0_3$ DF electron micrograph of the same area as Fig. 2(a), demonstrates that the $D0_3$ domains had grown considerably and that the $a/2\langle 100\rangle$ APBs gradually disappeared. In Fig. 2(c), it is also seen that the γ-brass particles occurred preferentially at $a/2\langle 100\rangle$ APBs. Shown in Fig. 2(d) is a (100_1) L–J DF electron micrograph, revealing that after being aged at 500 °C for 20 min, the size of the L–J precipitates was increased significantly. With increasing the aging time at 500 °C, the γ-brass particles grew rapidly and their morphology changes from cubic to irregular shape, as illustrated in Fig. 3(a). Fig. 3(b) is an SADP taken from a region marked as "A" in Fig. 3(a), indicating that the intensity of the reflection spots and streaking behavior of the L–J precipitates increased with increasing aging time. Fig. 3(c), a (100_1) L–J DF electron micrograph, reveals that the L–J precipitates grew considerably and the L–J precipitates surrounding the γ-brass particles were much larger than those away from γ-brass particles. Fig. 3(d) is a $(\bar{1}11)$ $D0_3$ DF electron micrograph, showing that the $D0_3$ domains have grown to reach a complete grain. Apparently, the microstructure of the alloy present at 500 °C was a mixture of (γ-brass + L–J + $D0_3$) phases. It is noted here that the coexistence of the (γ-brass + L–J) phases has never been observed by previous workers in the Cu–Al–Mn alloy systems before.

Shown in Fig. 4(a) is a (100_1) L–J DF electron micrograph of the alloy aged at 600 °C for 1 h and then quenched, indicating that the coexistence of (γ-brass + L–J) phases could also be observed. However, it is clearly seen in Fig. 4(a) that two types of L–J precipitates could be detected: one is the larger L–J precipitates surrounding the γ-brass particles which were existent at the aging temperature, and the other is the extremely fine L–J precipitates (the size being comparable to that observed in the as-quenched alloy) which were formed during quenching from the quenching temperature. Fig. 4(b) and (c) show $(\bar{1}11)$ and (002) $D0_3$ DF electron micrographs, clearly exhibiting small quenched-in $D0_3$ domains and well-grown B2 domains, respectively. This indicates that the microstructure of the alloy present at 600 °C was a mixture of (γ-brass + L–J + B2) phases. TEM observations indicated that the (γ-brass + L–J + B2) was preserved up to 675 °C. However, when the alloy was aged at 700 °C and then quenched, the microstructure is similar to that observed in the as-quenched alloy. This indicates that the microstructure existing at 700 °C or above is the single disordered β phase.

Based on the preceding results, it is obvious that the as-quenched microstructure of the present alloy was $D0_3$ phase containing extremely fine L–J precipitates. This is different from that examined by other workers in the Cu–25at.%Al–(0–8)at.%Mn alloys, in which they reported

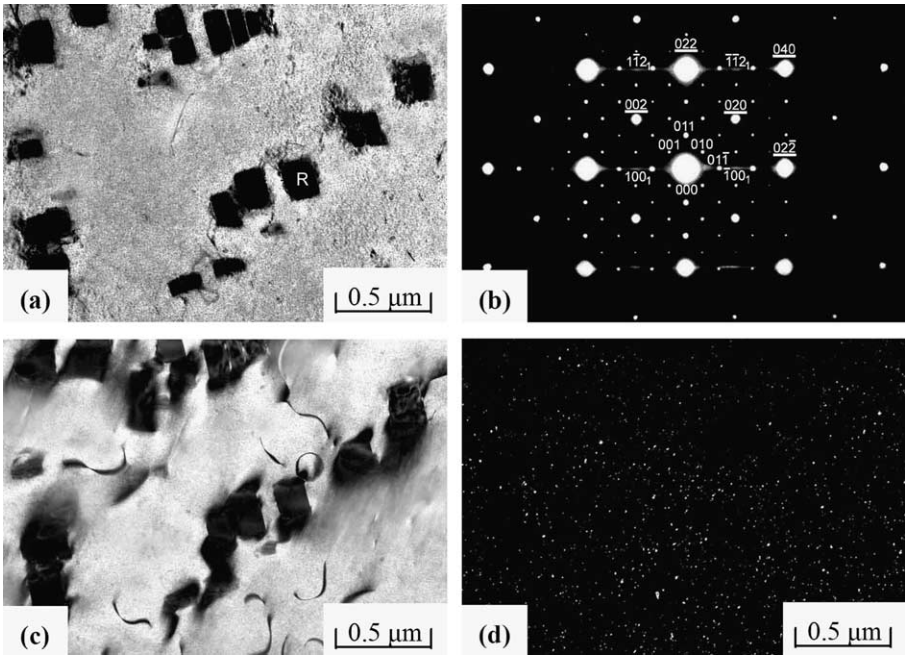

Fig. 2. Electron micrographs of the alloy aged at 500 °C for 20 min: (a) BF, (b) an SADP. The zone axis of the $D0_3$ phase is [100] ($\underline{hkl} = D0_3$, $hkl_1 = $ L–J phase and $hkl =$ γ-brass), (c) and (d) $(\bar{1}11)$ $D0_3$ and (100_1) L–J DF, respectively.

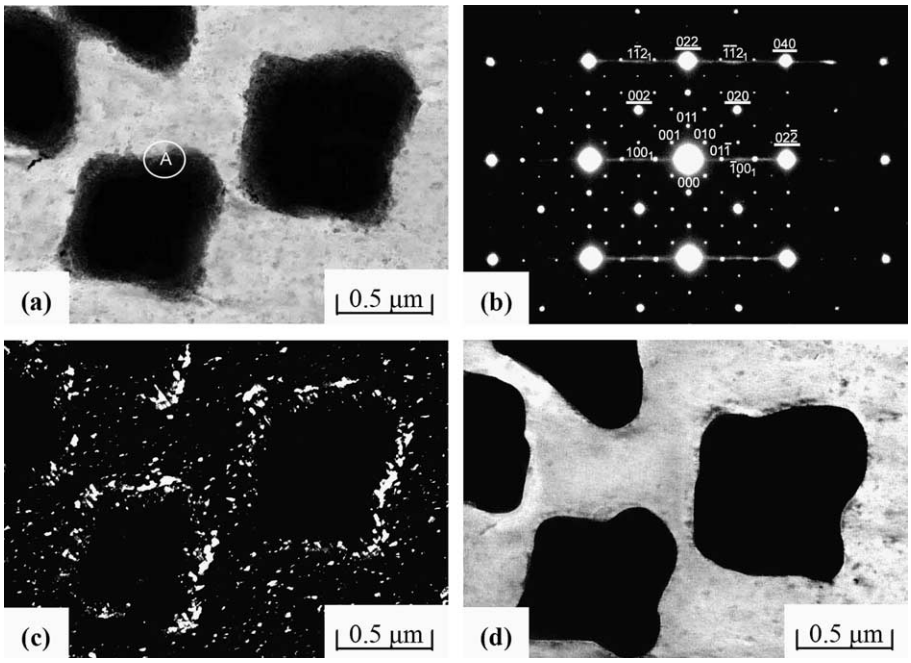

Fig. 3. Electron micrographs of the alloy aged at 500 °C for 2 h: (a) BF, (b) an SADP. The zone axis of the $D0_3$ phase is [1 0 0] ($\underline{hkl} = D0_3$, hkl_1 = L–J phase and hkl = γ-brass), (c) and (d) ($1\,0\,0_1$) L–J and ($\bar{1}\,1\,1$) $D0_3$ DF, respectively.

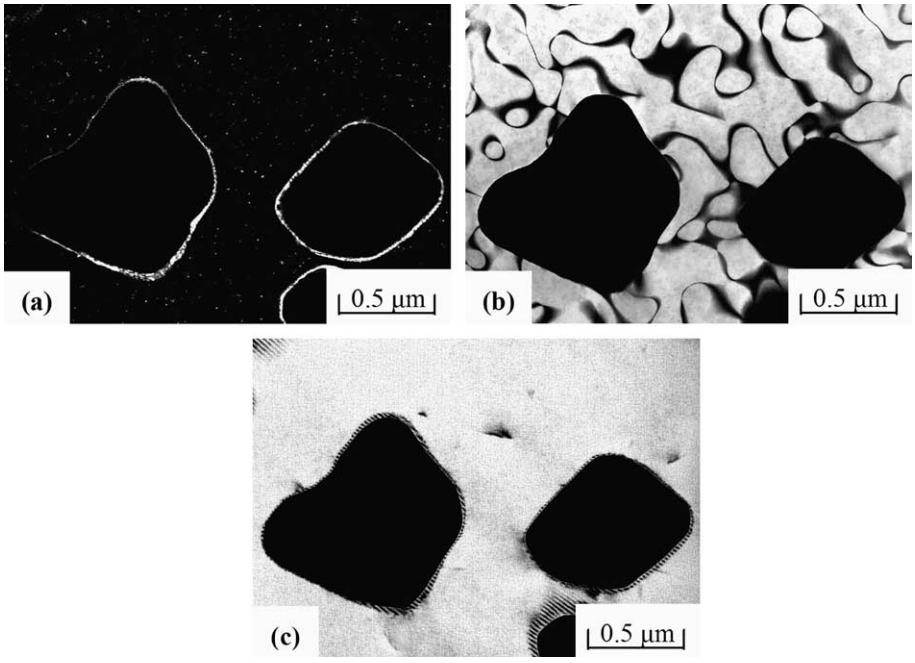

Fig. 4. Electron micrographs of the alloy aged at 600 °C for 1 h: (a) ($1\,0\,0_1$) L–J DF, (b) and (c) ($\bar{1}\,1\,1$) and (0 0 2) $D0_3$ DF, respectively.

that the as-quenched microstructure was single $D0_3$ phase [1–3]. Here, it is worthwhile pointing out that the extremely fine L–J precipitates had also been detected and identified by the present workers in the as-quenched $Cu_{2.2}Mn_{0.8}Al$ and Cu_2MnAl alloys [11,17]. However, compared to our previous studies, it is clear that the amount of the L–J precipitates existing in the present alloy is less than that observed in the previous alloys. It seems to imply that the higher Mn content in the $Cu_{3-x}Mn_xAl$ alloys may enhance the formation of the extremely fine L–J precipitates within the matrix during quenching.

The coexistence of (γ-brass + L–J) phases is a remarkable feature in the present study, which has never been observed by other workers in the Cu–Al–Mn alloy systems before. In order to clarify this feature, an STEM-EDS study was performed. Fig. 5(a) and (b) represent two

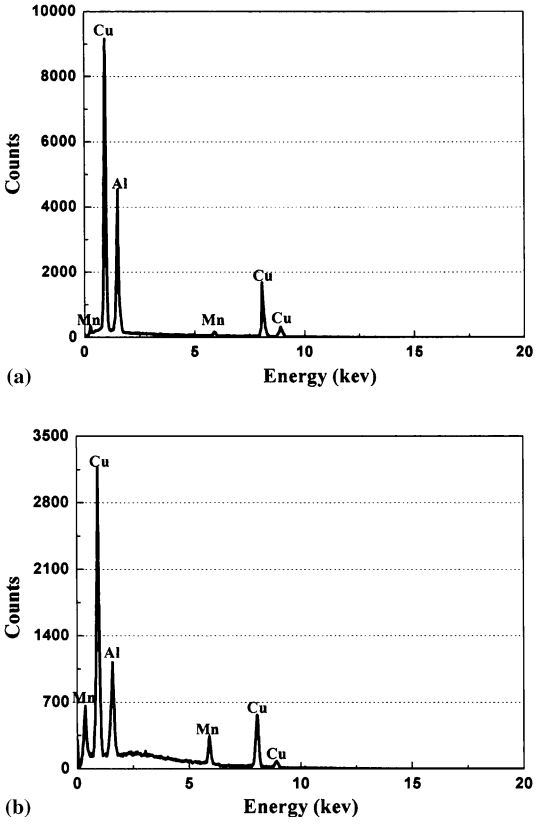

Fig. 5. Two typical EDS spectra obtained from (a) a γ-brass particle, and (b) an L–J precipitate in the alloy aged at 500 °C for 2 h, respectively.

typical EDS spectra for a γ-brass particle and an L–J precipitate in the alloy aged at 500 °C for 2 h, respectively. The quantitative analyses revealed that the atomic percentages of the alloying elements in the γ-brass particle and L–J precipitate were Cu–29.84at.%Al–2.76at.%Mn and Cu–17.52at.%Al–15.34at.%Mn. It is clear that the concentration of Mn in the γ-brass is much less than that in the as-quenched alloy. Therefore, it is expected that along with the growth of γ-brass particles, the surrounding regions would be enriched in Mn. The enrichment in Mn would cause the Mn-rich L–J precipitates to form at the regions contiguous to the γ-brass particles, as observed in Figs. 3(c) and 4(a).

4. Conclusions

1. In the as-quenched condition, the microstructure of the Cu–25at.%Al–7.5at.%Mn alloy was $D0_3$ phase containing extremely fine L–J precipitates.
2. When the as-quenched alloy was aged at temperatures ranging from 500 °C to 675 °C, γ-brass particles were found to occur preferentially at APBs. With increasing aging time, the L–J precipitates started to appear at the regions contiguous to the γ-brass particles. The coexistence of (γ-brass + L–J) phases has never been observed by other workers in the Cu–Al–Mn alloy systems before.

Acknowledgments

The authors are pleased to acknowledge the financial support of this research by the National Science Council, Republic of China under Grant NSC93-2216- E009-016. They are also grateful to M.H. Lin for typing the manuscript.

References

[1] Marcos J, Vives E, Castán T. Phys Rev B 2001;63:224418.
[2] Kainuma R, Satoh N, Liu XJ, Ohnuma I, Ishida K. J Alloy Compd 1998;266:191.
[3] Prado M, Sade M, Lovey F. Scripta Metall Mater 1993;28:545.
[4] Obradó E, Frontera C, Maoñsa L, Planes A. Phys Rev B 1998;58:14245.
[5] Counioux JJ, Macqueron JL, Robin M, Scarabello JM. Scripta Metall 1988;22:821.
[6] Miettinen J. Calphad 2003;27:103.
[7] Dvorack MA, Kuwano N, Polat S, Chen H, Wayman CM. Scripta Metall 1983;17:1333.
[8] Kozubski R, Soltys J. J Mater Sci 1982;17:1441.
[9] Singh J, Chen H, Wayman CM. Scripta Metall 1985;19:887.
[10] Dutkiewicz J, Pons J, Cesari E. Mater Sci Eng 1992;A158:119.
[11] Jeng SC, Liu TF. Metall Mater Trans 1995;26A:1353.
[12] Kuwano N, Wayman CM. Metall Trans 1984;15A:621.
[13] Wu CC, Chou JS, Liu TF. Metall Trans 1991;22A:2265.
[14] Tan J, Liu TF. Mater Chem Phys 2001;70:49.
[15] Swann PR, Duff WR, Fisher RM. Metall Trans 1972;3:409.
[16] Allen SM, Chan JW. Acta Metall 1976;24:425.
[17] Chu KC, Liu TF. Metall Mater Trans 1999;30A:1705.